Thermal Design of the Tropospheric Emission Spectrometer Instrument

José I. Rodriguez
Jet Propulsion Laboratory, California Institute of Technology

ABSTRACT

The Tropospheric Emission Spectrometer (TES) is a cryogenic instrument which will be launched on NASA's Earth Observation System (EOS) Chemistry Platform in the year 2003. The overall mission lifetime for the instrument is 5 years with an additional period of 2 years required for ground test and calibration. The EOS Chemistry Platform will be placed in a sun-synchronous near-circular polar orbit with an inclination of 98.2 degrees and a mean altitude of 705 km. The overall objective of TES is the investigation and quantification of global climate change, both natural and anthropogenic. It is a high resolution infrared imaging (1x16 pixels) Fourier Transform Spectrometer with spectral coverage of 3.3-15.4 µm at a spectral resolution of 0.10 cm^{-1} or 0.025 cm^{-1} intended for the measurement and profiling of essentially all infrared-active molecules present in the Earth's lower atmosphere (0-30^{+} km).

The thermal design provides four temperature zones required by the instrument, namely 65 K, 180 K, 230 K and 300 K. The detectors are cooled by mechanical pulse-tube coolers to 65 K and a two-stage passive cooler provides cooling for the interferometer optics at 180 K. Detector pre-amplifier electronics requires 230 K as well as the optics filter wheel actuators. The remaining electronics including the mechanical cooler compressor requires ambient temperatures near 300 K.

The thermal control system consists of passive and active elements to maintain the instrument within allowable flight temperature limits. Passive thermal control includes multi-layer insulation (MLI) blankets, thermal straps, and surface coatings to manage the transfer of waste energy from sources through structures and ultimately to radiators. Active thermal control employs constant conductance heat pipes (CCHPs), loop heat pipes (LHPs) and both open-loop and close-loop heater control systems. Operational and replacement heaters are used in the instrument science mode and survival heaters are used in the safe and survival modes. LHPs are used to transport waste heat

from components to the heat rejecting radiator surfaces. Detailed description of LHPs can be found elsewhere [1-8]. Steady state and transient performance test results of a propylene LHP of similar design to the TES LHPs is presented in Refs. 9 and 10. This paper describes the instrument thermal requirements, thermal design and analysis approach, key drivers for the design process and analysis results.

INTRODUCTION

The TES instrument, designed and built by the Jet Propulsion Laboratory for NASA, will fly onboard the EOS Chemistry spacecraft scheduled to be launch June 2003 aboard a Delta II vehicle from Vandenberg Air Force Base in California. TES is being developed with significant subcontractor support building critical hardware such as the composite optical bench and support structure, passive cooler, mechanical pulse-tube coolers, loop heat pipes, pointing and interferometer control subsystems and beryllium optics. The EOS Chemistry project is managed by NASA's Goddard Space Flight Center. As the third mission of NASA's EOS Program, the Chemistry satellite hosts a suite of scientific instruments designed to make the most comprehensive measurements ever undertaken of atmospheric trace gases. The satellite's orbit was selected to allow measurements to be taken at all latitudes with complete coverage of the entire globe in 16 days. The EOS Chemistry instruments HIRDLS, MLS, OMI, and TES have unique and complementary capabilities to map on a global scale data on the Earth's atmosphere. TES measurements will help determine local atmospheric temperature and humidity profiles, local surface temperatures, and local surface reflectance and emittance. TES observations will also be used to study volcanic emissions for hazard mitigation, indications of the chemical state of the magma, eruption prediction, and quantification of the role of volcanoes as sources of atmospheric aerosols. A detailed description of TES and its science capabilities is found in Ref. 11. EOS Chemistry is a component of national and international efforts to understand the Earth's

atmosphere. An artist's conception of the EOS Chemistry spacecraft on orbit is shown in Fig. 1. The spacecraft without external MLI blankets is shown in Fig. 2.
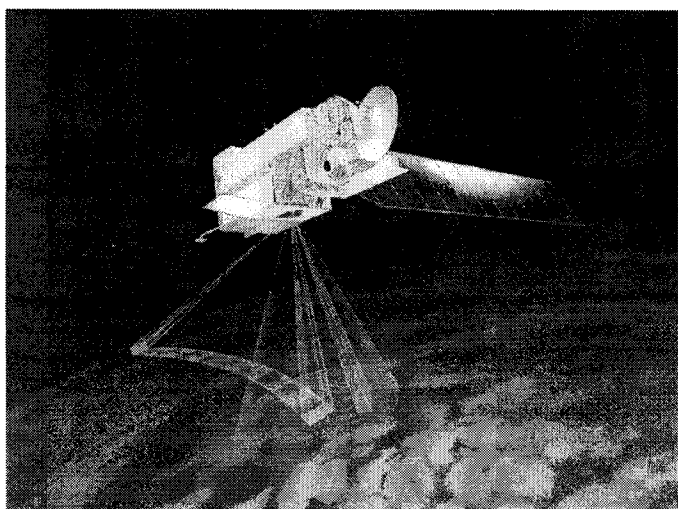

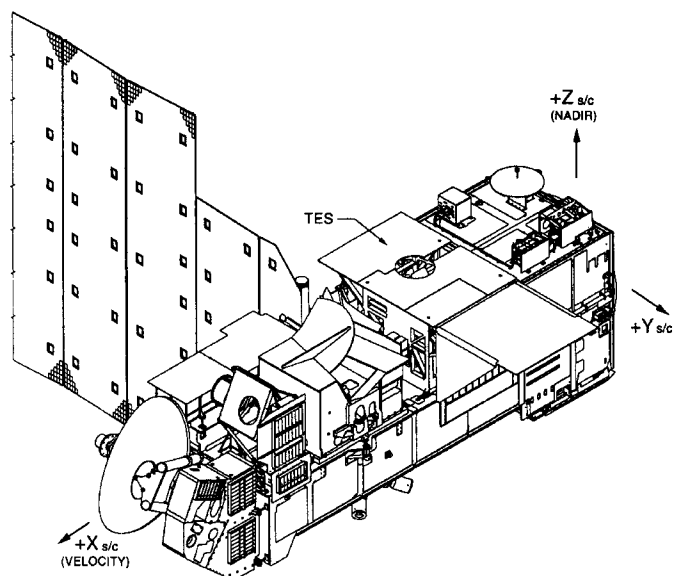Figure 1. EOS Chemistry spacecraft in orbit

Figure 2. EOS Chemistry spacecraft configuration

Due to the challenging thermal requirements, tight mass and power budgets, restrictive spacecraft accommodations and widely varying mission conditions, the TES instrument posed a challenging thermal design opportunity. Further compounding this challenge was the extremely tight dimensional stability requirements for the optical elements mounted on the optical bench operating near 180 K.

INSTRUMENT DESCRIPTION

TES has capability to make both nadir and limb observations. In the limb mode, it has a height resolution

of 2.3 km, with coverage from 0 to 34 km. In the nadir modes, it has a spatial resolution of 0.53 by 5.3 km with a swath of 5.3 by 8.5 km. TES is a pointable instrument and can access any target within 45 degrees of local vertical, or produce regional transects up to 885 km length without any gaps in coverage. This instrument makes use of both the natural emission of the surface and atmosphere and reflected sunlight, thereby providing day-night coverage anywhere on the globe.

The heart of the TES instrument is four focal plane arrays located in two separate focal-plane opto-mechanical assemblies (FPOMAs) that are cooled to 65 K by a pair of mechanical pulse-tube coolers. The interferometer optics including the FPOMA housings are maintained at 180 K by means of the passive cooler second stage. The first stage intercepts parasitic heat leaks from the surrounding environment at 300 K. The optics and translator housing contain all the interferometer optics including the retro-reflector. The retro-reflector is a double cube corner that is mounted on a translator carriage that traverses back and forth, continuously changing the optical path length. The instrument optical schematic diagram with temperature zones is shown in Fig. 3.
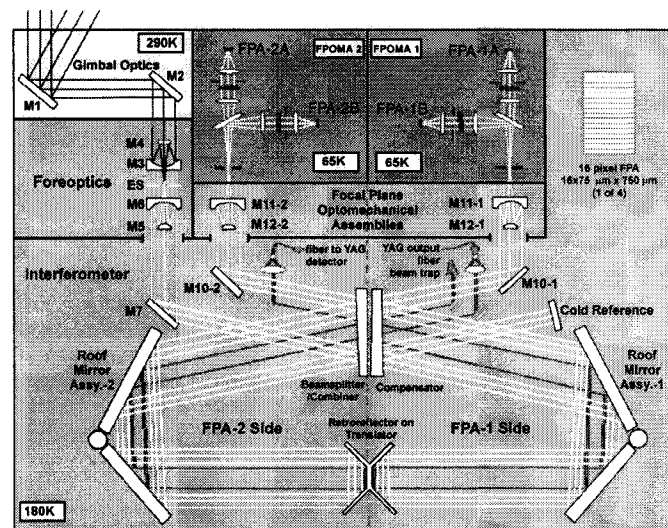

Figure 3. Instrument optical schematic diagram with temperature zones

The instrument structure is built primarily from advanced composite materials as well as the optical bench and passive cooler. The instrument envelope is 1.4 m by 1.3 m by 1.35 m with the earthshade stowed and 3.04 m by 1.3 m by 1.35 m with the earthshade deployed. The allocated mass and average operating power is 350 kg and 334 W respectively. The heat load from the interferometer to the second stage radiator of the passive cooler is 22 W at 180 K. The instrument design incorporates both passive and active thermal control techniques to reject the waste heat. The mechanical cooler design heat load is 750 mW at 62 K. Electronic

2

assemblies are mounted to the base structure and the +X side panel. The radiometric and spatial calibrators are mounted to a composite beam spanning the structure near the pointing mirror. The pointing mirror mounts to a gimbal assembly in the +Z side of the support structure. The field of view is 45° for cross-track and +45° to −72° along-track. Isometric views from the solid CAD model with the earthshade stowed and deployed are shown in Figs. 4 and 5, respectively. The instrument configuration drawing is shown in Fig. 6.
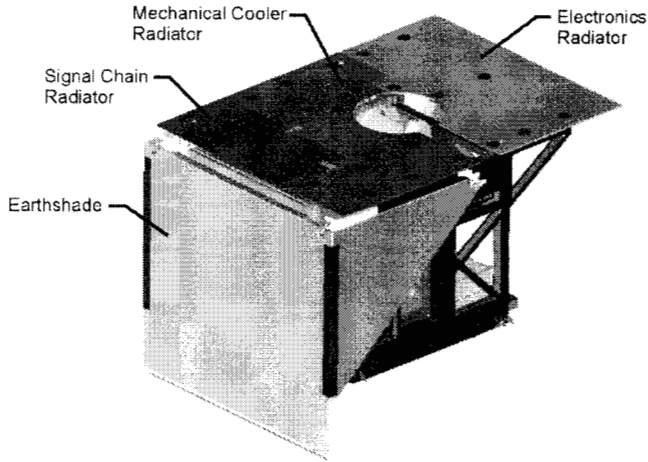

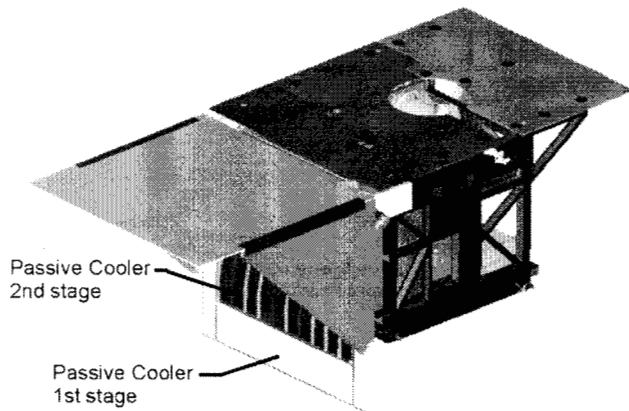
Figure 4. TES instrument with earthshade stowed

Figure 5. TES instrument with earthshade deployed

SPACECRAFT ENVIRONMENTS

The key drivers for the TES thermal design are as follows:

- Orbit parameters: sun-synchronous, near-circular orbit, 705 km altitude, 1:45 pm ± 15 min ascending node, 98.21 degree orbit inclination

- Spacecraft interface temperatures: 0/+30°C for science and safe mode and −20/+50°C during survival mode

- Heat transfer to spacecraft is limited to 15.5 W/m², which includes radiation and conduction heat transfer

- Spacecraft accommodations may add a maximum of 3 W/m² heat flux to the passive cooler radiators

- Survival heater power is limited to 30% of allocated operational mode average power

The parameters and conditions of each spacecraft state defining the hot and cold mission environments, safe and survival spacecraft attitudes and the solar vector to orbit plane (beta) angle is shown in Table 1. The environmental constants used are defined in Table 2. Fig. 7 defines the science and survival orbits.

Table 1. EOS Chemistry spacecraft mission environments

S/C state	Beta angle (degrees)		S/C Attitude	Description
	hot	cold		
Launch	varies	varies	varies	Includes ascent, coast, orbit insertion to power on. Earth shade stowed config.
Science	16	36	+Z local vertical (nadir pointing)	Earth shade deployed
Safe	16	36	+Z local vertical (nadir pointing)	Earth shade deployed
Survival	NA	16	-X solar inertial (sun pointing). S/C rolls about X-axis at 2 ± 0.2 rev/orbit	Earth shade deployed

Table 2. Mission environment parameters

Parameter	Cold Case	Hot Case
Solar Flux	1290 W/m²	1420 W/m²
Albedo	0.275	0.375
Earth IR	222 W/m²	243 W/m²

THERMAL DESIGN REQUIREMENTS

The instrument thermal requirements along with spacecraft mission environments pose a very challenging thermal and cryogenic design problem. Spacecraft requirements dictate that the instrument thermal control be independent of the platform.
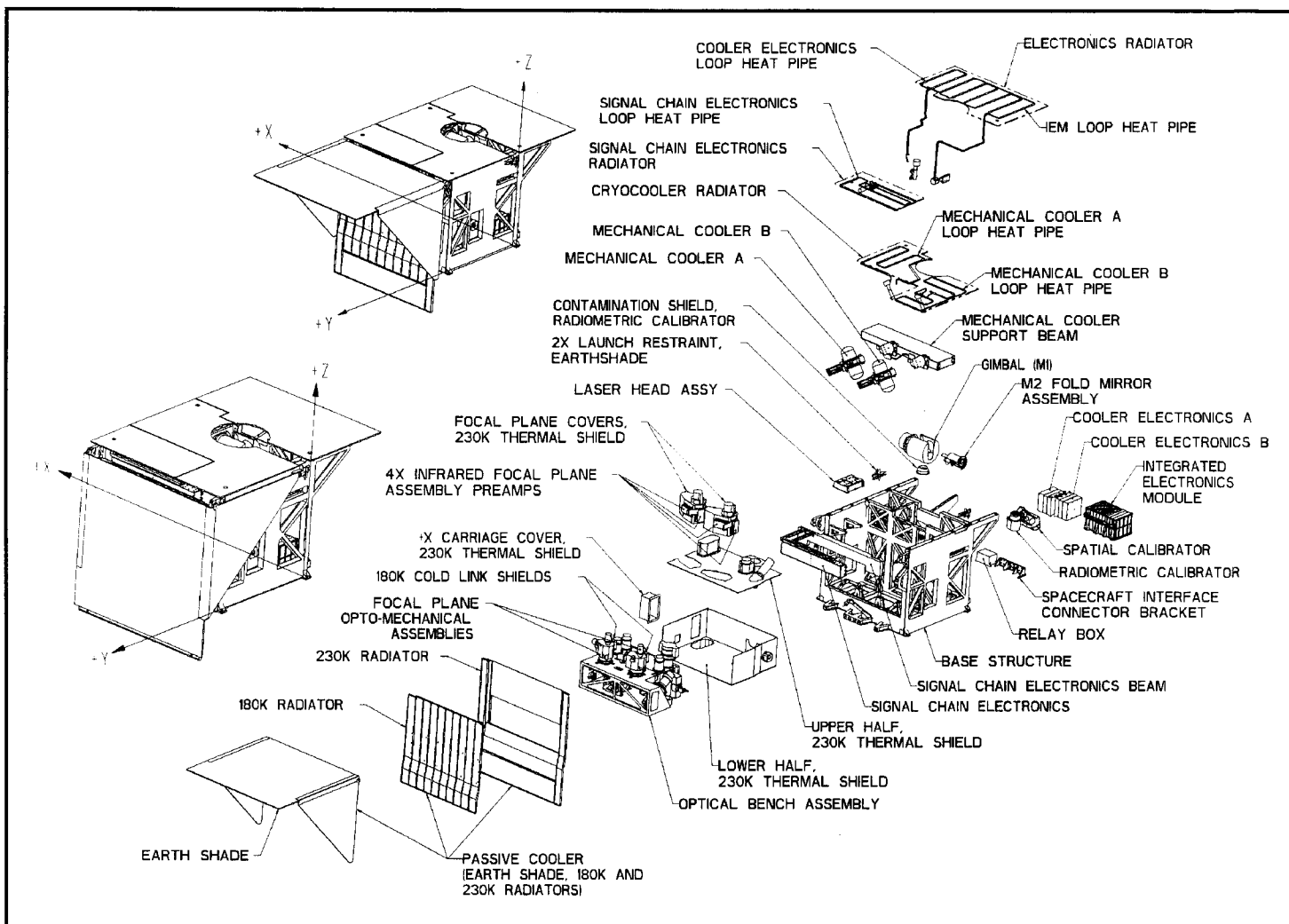
Figure 6. Instrument configuration.

This leads to the use of MLI blankets and titanium thermal isolator mounts to provide the required thermal isolation. In addition, passive nadir pointing heat rejection radiators are required to reject the instrument power dissipation. To provide cooling to the interferometer at 180 K, a passive two-stage cooler is required with cold radiators facing the anti-sun side (+Y) of the spacecraft.

The key temperature control requirements are listed in Table 3. The instrument power dissipation assemblies are listed in Table 4. The instrument exterior is covered with MLI blankets with the exception of the nadir viewing and passive cooler deep space viewing radiators and the earthshade.

THERMAL DESIGN

The overall instrument thermal design focuses on three thermal control zones; (1) focal plane temperature zone at 65 K for detectors and focal plane optics, (2) optical bench near 180 K for the interferometer optics including the retro-reflector and FPOMAs and (3) room temperature zone near 300 K for the mechanical cooler compressors, integrated electronics module, signal chain electronics, laser head assembly, mechanical cooler electronics and radiometric and spatial calibrators. The 65 K zone within each FPOMA is provided by means of a mechanical pulse-tube cooler. An all-aluminum flexible S-shape cold link is used to thermally couple the cooler coldblock to the focal planes. The 180 K zone is provided by means of the second stage radiator of the passive cooler. The 300 K zone is achieved by means of nadir facing radiators.

The 65 K zones are contained within each FPOMA. The FPOMA housing interface temperature is maintained at 177±2 K by means of the optical bench open-loop temperature control.
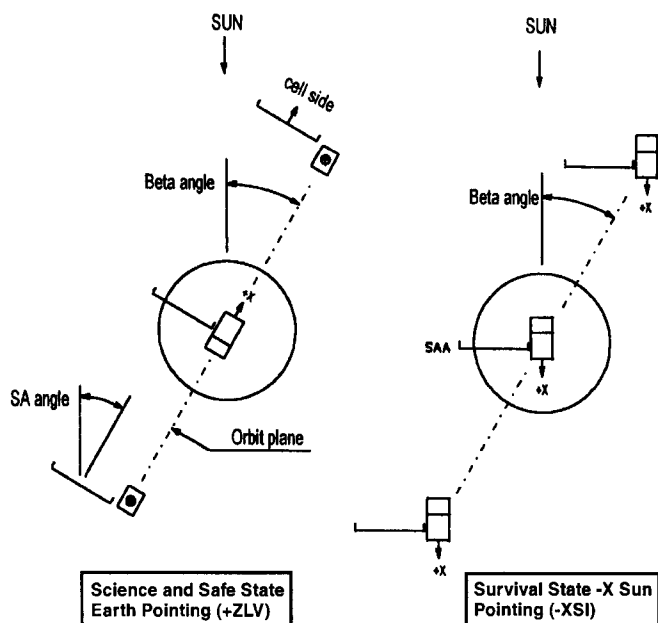
4

Figure 7. Chemistry spacecraft science and survival orbit definitions

Table 3. Allowable flight temperature requirements

| | Allowable Flight Temperatures (°C) | | | |
| | Non-operating | Operating | | |
	Survival	Orbit Var.	Grad	Design
IEM [1]	-25/50	7		0/50
Signal Chain Electronics	-25/50	5		0/35
Cooler Electronics	-25/50	5		0/50
Laser Head Electronics	-25/50			0/35
Mech Cooler Compressor	-25/50			0/35
Trans. Actuator/ Encoder	-25/50			-10/40
Roller Bearings	200K/300K			230K/250K
Optical Bench (Optics Hsg)	165K/300K	±2 K	20	177 ± 2 K
Filter Wheel	65K/300K			65K/90K
Filter Wheel Actuator	-50/50			-33/50
Detectors	64K/300K	±1 K		65±1K
Detector Pre-Amplifier	250/323K			230K/270K
Earth Shade Mechanism	-50/50			-43/30
PCS [2] Roll Motor/Encoder	-25/50	5		-10/50
PCS Pitch Motor/Encoder	-25/50			-10/50
PCS Mirror	-25/50			-25/50
Radiometric Calibrator	-25/50			0/50

1. Integrated Electronics Module
2. Pointing and Control Subsystem

The parasitic heat leak to the 65 K zone is minimized by means of two concentric fiberglass tubes for thermal isolation and a single gold coated radiation shield between the 65 K zone and the FPOMA housing. Figs. 8-10 illustrate the design concept. The S-link and the mechanical cooler coldblock are covered with 20 layer MLI blankets. The estimated total parasitic heat leak to the cooler cold block is less than 600 mW at 62 K.

A passive two-stage cooler is used to provide cooling for the optical bench assembly below 180 K. The first stage provides cooling to a thermal shield near 230 K which completely surrounds the optics housing to intercept parasitic heat leaks from the warm structure and instrument electronics. A thermal schematic of the optical bench and passive cooler is shown in Fig. 11.

Table 4. Equipment average power dissipation

	Component	Power (Watts)*
Electronics Radiator	IEM	100.8
	Mech Cooler Electronics 1	16.0
	Mech Cooler Electronics 2	16.0
Signal Chain Radiator	Signal Chain Electronics 1 & 2	28.7
	Laser Head Assembly	5.9
Mechanical Cooler Radiator	Mechanical Cooler Compressor 1	43.5
	Mechanical Cooler Compressor 2	43.5
Passive Cooler	Translator Actuator/Encoder	4.25
	Filter Wheel Actuators (4 ea. / 0.16 W)	0.756
	Optical Bench Heaters	15.6
	Detector Pre-amplifiers (4 ea. / 0.9 W)	4.32
	Trans. Bearing Assy Heaters (7 ea./0.19W)	1.33
Other	PCS Roll and Pitch Motor/Encoder	0.6
	Detector (4 each @ 30 mW)	0.144
	Radiometric Calibrator	3.5
Total Power Dissipation		284.9

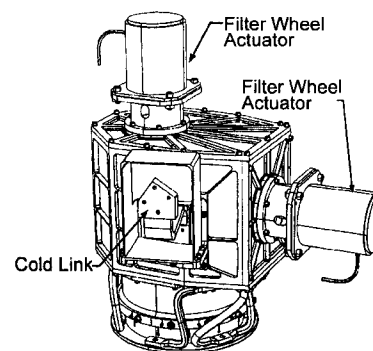* Power dissipation includes margin

Figure 8. Focal-plane opto-mechanical assembly housing

The passive cooler makes use of the spacecraft anti-sun side to obtain a clear field of view of deep space. The optical bench temperature at the FPOMA interface is control by means of open-loop temperature controller with heater power control authority of 15 watts maximum.

This provides a 10 K control range over the life of the instrument. It is expected that at BOL, the heater controller will be operating at full power and will gradually degrade as the instrument ages.
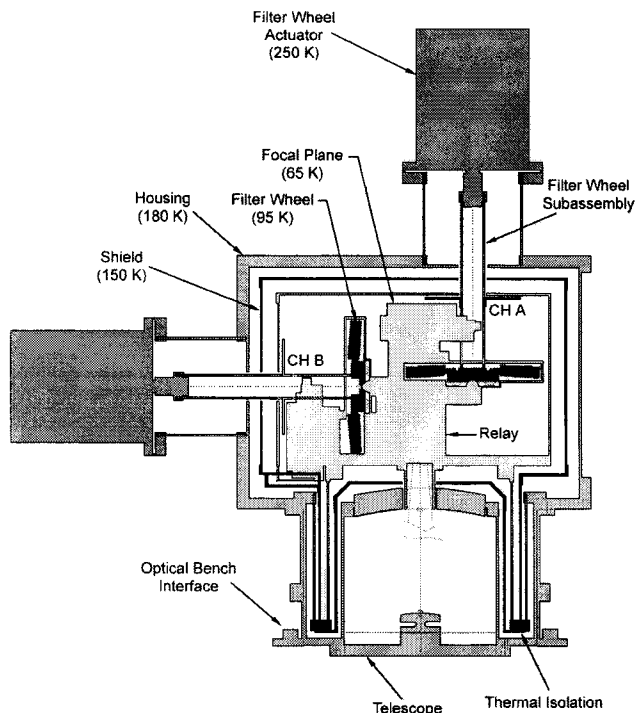

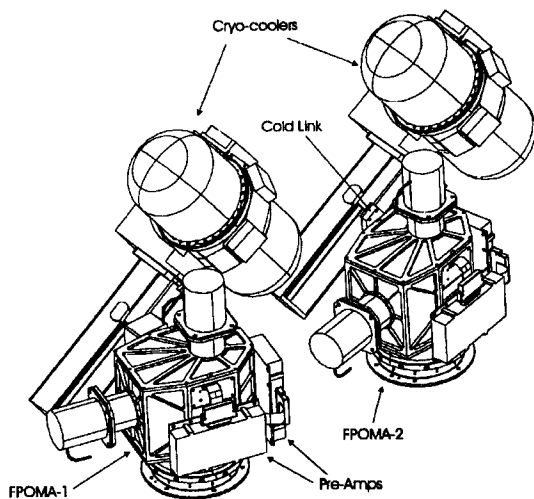Figure 9. Focal-plane opto-mechanical assembly cross-section

Figure 10. Mechanical pulse-tube coolers with FPOMAs

The optical bench is constructed from K13C2U composite laminates, which is a high modulus composite material with good thermal conductivity, similar to aluminum, and relatively low CTE. Tight dimensional

stability requirements and thermal design constraints were achieved using this high modulus dimensionally stable composite. All optical mounts and various bolted interfaces were made from Invar for compatibility with a low CTE bench. The optical bench is mounted to the instrument base structure with low conductance boron struts. Fig. 12 illustrates the strut design. Fig. 13 shows the optical bench assembly.
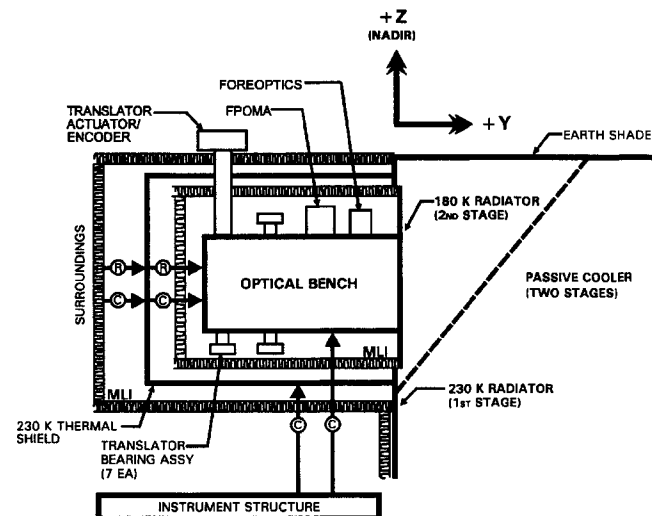

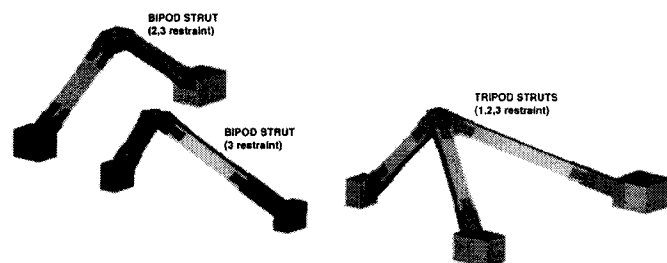Figure 11. Optical bench thermal schematic

Figure 12. Optical bench support struts

The thermal shield is constructed from aluminum honeycomb panels with K13C2U composite laminate facesheets. These panels provide suitable in-plane conductance to transfer the intercepted heat to the first stage radiator with an acceptable temperature gradient. All heater and temperature sensor wires are heat sunk to the 230 K thermal shield. The 230 K thermal shield including the first stage radiator are supported from the instrument base structure using fiberglass supports. An MLI blanket completely surrounds the optical bench including the backside of the second stage radiator. The optical bench was designed for a 15 K maximum temperature gradient from the backside to the second stage radiator surface.

The thermal shield surrounding the optical bench is also covered with MLI as well as the backside of the first stage radiator. Both the first and second stage radiators are constructed from K1100 composite laminates, which have a high in-plane thermal conductivity. Both radiators were designed with fin efficiencies exceeding 0.95. These radiators have black painted (Z307) open-cell aluminum honeycomb bonded to the external surface to enhance the effective emissivity. Measurements made on test samples show effective emissivities greater than 0.95 from room temperature to 130 K.
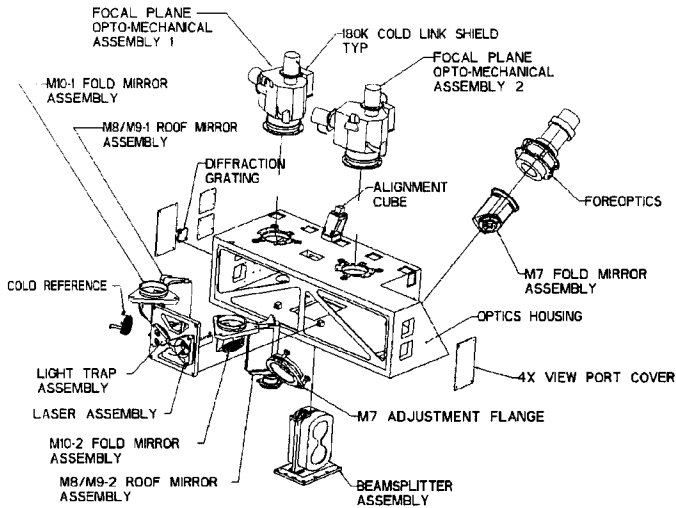
Figure 13. Optical bench assembly

The deployable passive cooler cover serves as an earthshade, protecting the radiators from direct Earth IR. The exterior surface of the earthshade is painted white to reduce its temperature and thus minimize its IR emission to the first and second stage radiators. The interior surface is specular vapor deposited aluminum (VDA) to minimize the combination of emissivity, absortivity and solar scattering. The solar specularity requirement is 0.98 begining-of-life (BOL), an important factor in the overall heat rejection capacity of the passive cooler. The earthshade is constructed using aluminum honeycomb core with M55J composite laminate facesheets. Table 5 shows the thermal optical surface properties for the passive cooler.

Thermal control for the 300 K zone uses a combination of CCHPs and LHP systems to transport and manage the equipment power dissipation. The thermal design system uses five CCHPs and LHPs each to transport waste heat from the heat dissipating components to the instrument nadir radiator panels. The nadir radiators are comprised of three separate thermally isolated panels; (1) mechanical cooler radiator for rejecting waste heat from both mechanical cooler compressors, (2) electronics radiator for rejecting waste heat from the IEM and mechanical cooler electronics and (3) signal chain radiator to reject heat from signal chain and laser head

electronics. The LHP systems use propylene as the working fluid and are based on single evaporator with single-sided heat input and condenser designs.

Table 5. Passive cooler surface properties

Item	Surface Type	Surface Properties		Surface Specularity			
		BOL (α / ε)	EOL (α / ε)	IR		Solar	
first and second stage rad 230/180K	open-cell Aluminum honeycomb Z307 black	.95/.95	.95/.95	-	-	-	-
Earth shade interior	VDA (specular)	.08/.04	.13/.04	.99	.97	.98	.95
Earth shade exterior	white paint (S13G/LO)	.20/.88	.35/.88	-	-	-	-

The evaporators are attached to the power dissipation components with a bolted interface and the condensers are bonded to the radiator panels using EA9394 adhesive. Fig. 14 shows the thermal design approach for the mechanical cooler electronics. A similar design is used for the IEM and signal chain electronics, where CCHPs are used to transport the waste heat from the equipment to the evaporators. Fig. 15 shows the complete IEM LHP.
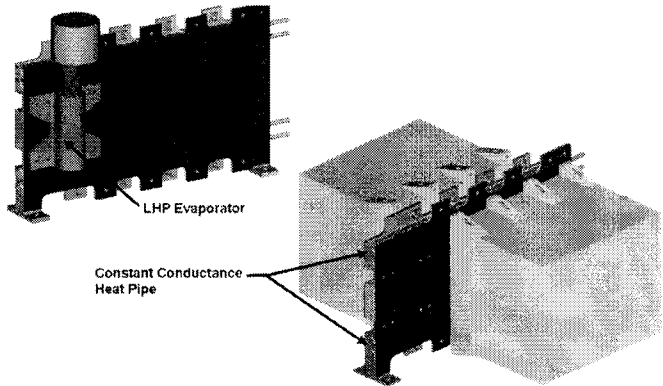

Figure 14. Mechanical cooler electronics with LHP evaporator

All LHPs make use of flexible sections for the vapor and liquid return lines at both transitions to the evaporator and condenser. This facilitates integration of the LHPs to the equipment and permits buildup of large structural fabrication tolerances without problems. Fig. 16 shows the radiator panels with all the LHPs. Ammonia filled CCHPs are used to collect and transport waste heat from the IEM and mechanical cooler electronics to the LHP evaporator heat lift interface. The radiator panels are constructed using an aluminum honeycomb core

structure with thin aluminum high conductivity facesheets (AL1100). The radiators are painted white to minimize the solar absorbed flux. The radiator panels which incorporate the LHP condenser layout were designed to produce high radiator fin efficiencies resulting in overall radiator effectiveness greater than 0.95.
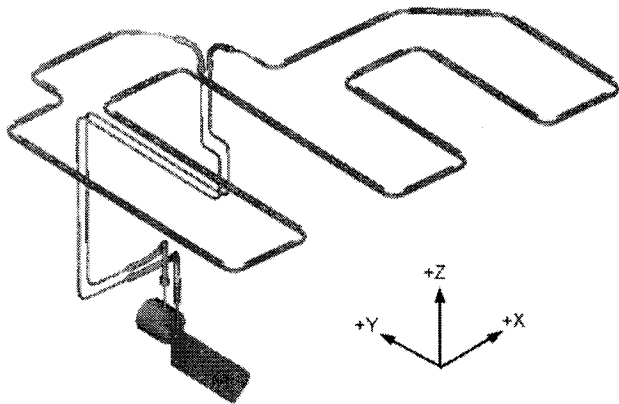

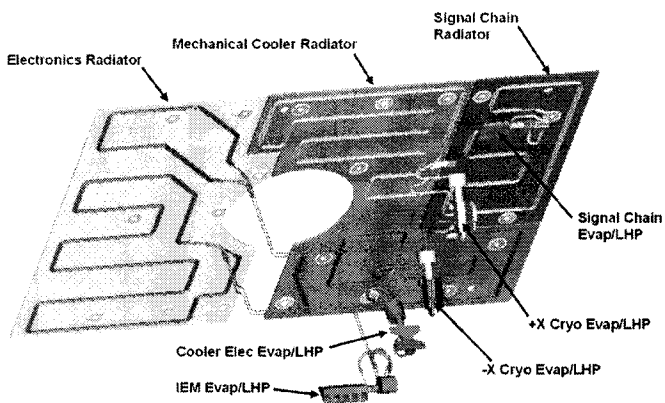Figure 15. IEM loop heat pipe with condenser line

Figure 16. Nadir radiators with loop heat pipes

In survival mode the instrument is powered off, the orbit average effective radiator sink temperature drops from -32°C to -92°C and a limited amount of power is available to maintain equipment temperatures within the allowable flight non-operating limits. While in this mode, the LHPs are shut-off to prevent heat transport from the equipment items to the cold radiator panels. This is a key thermal control requirement needed to meet the stringent spacecraft survival power requirements. The use of LHPs on TES has facilitated the mechanical configuration layout for the entire instrument and permits the thermal decoupling of the components from the radiators in survival mode.

THERMAL ANALYSIS

Instrument thermal analysis was performed using a reduced geometric math model (RGMM) developed with the thermal synthesizer system (TSS) software package and reduced thermal math model (RTMM) developed in SINDA/G format. The RGMM consist of 60 surfaces and the RTMM contains 125 thermal nodes. Isometric views of the RGMM are shown in Figs. 17-19.

Table 6. Instrument external surfaces

Item	Surface Type	Surface Properties	
		BOL (α / ε)	EOL (α / ε)
Electronic radiator	White paint (Hughes M-1)	0.08/0.91	0.15/0.91
Cryocooler radiator			
Signal chain radiator			
Gimbal trough MLI outer layer	1 mil carbon filled Kapton	0.93/0.78	0.93/0.78
Pointing mirror (M1/M2)	Gold surface	0.20/0.05	0.35/0.05
Gimbal shield, exterior	White paint (S13G/LO)	0.20/0.88	0.35/0.88
Gimbal shield, interior	Black paint (Dexter 463-3-8)	0.80/0.86	0.80/0.86
Gimbal motor	Bare AL 6061-T6	0.20/0.10	0.35/0.20
MLI outer layer (instrument ext. MLI)	3 mil aluminized Kapton	0.38/0.65	0.42/0.63
MLI effectiveness* (instrument ext. MLI)	15 layer-Mylar	0.025	0.035
MLI effectiveness* (between optical bench and 230K shield)	20 layer-Mylar	0.020	0.030
MLI effectiveness* (surrounding 230K shield)	20 layer-Mylar	0.030	0.040

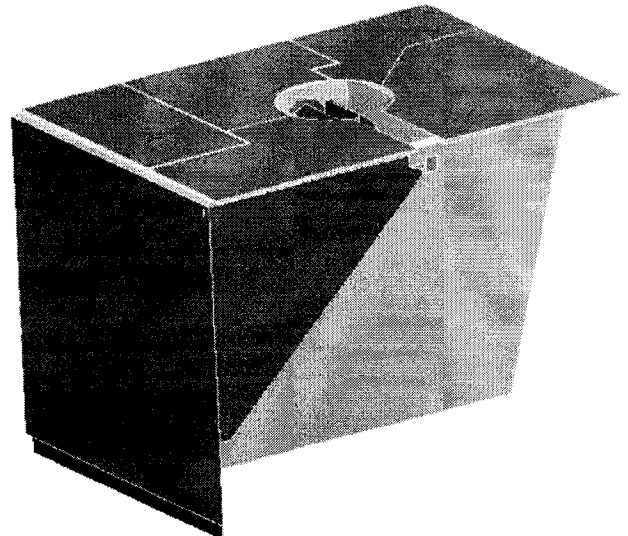* Values denote MLI effective emissivity

Figure 17. Instrument RGMM: earthshade stowed configuration

In parallel, an instrument detailed geometric math model (DGMM) and detailed thermal math model (DTMM) were developed to obtain increased fidelity in critical areas.

8

The DGMM contains some 2000 surfaces and the DTMM has 3000 thermal nodes. The RGMM and RTMM were delivered to the spacecraft integrator for inclusion in the overall spacecraft thermal analysis. From the spacecraft-level thermal analysis, environmental heat fluxes and infrared backloads were generated for inclusion in the stand-alone instrument models. The spacecraft integrator carried out a detailed specular analysis specifically for TES and provided the results to include in the instrument model.
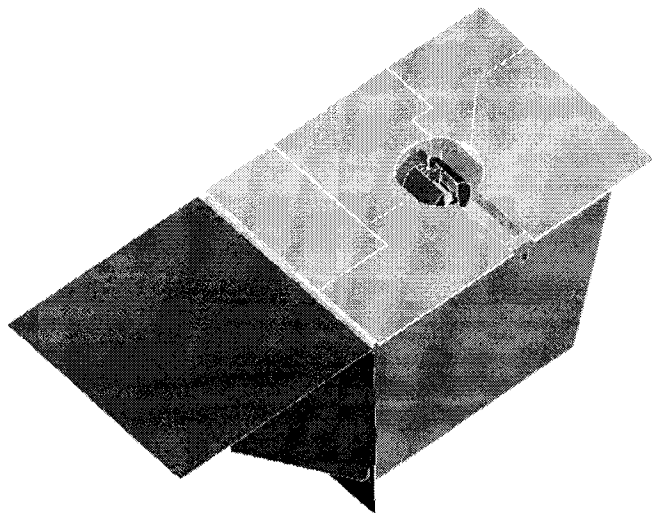

Figure 18. Instrument RGMM: earthshade deployed configuration
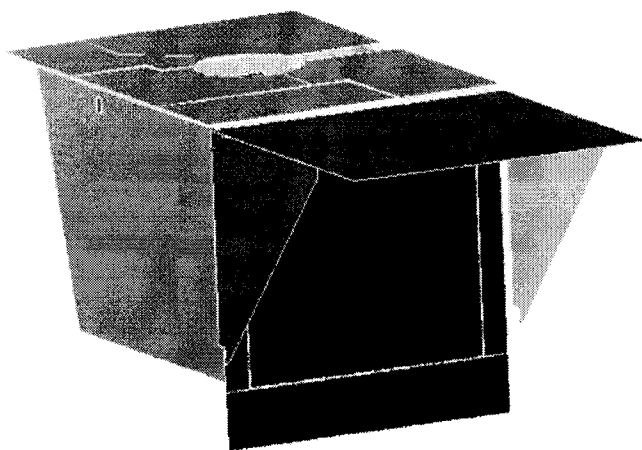
Figure 19. Instrument RGMM: passive cooler view

Early in the design process, very detailed unit level thermal models were developed to be able to carryout trade studies and identify the sensitivity of various parameters including geometry. These included models for the optical bench (see Fig. 20), focal-plane opto-mechanical assembly, pointing and control subsystem, interferometer control subsystem, passive cooler, retro-reflector, LHP evaporator and radiators with

condenser lines (see Figs. 21 and 22) and IEM with CCHPs.

Detailed models were also constructed for bonded joints and fittings to determine the effects of the anisotropic nature of composite materials. Composites can have relatively high in-plane conductivity; however, the through-thickness conductivity is always poor. These models were developed using SINDA85, SINDA/G, TSS, SINDA/3D, thermal analysis system (TAS) and Ansys.
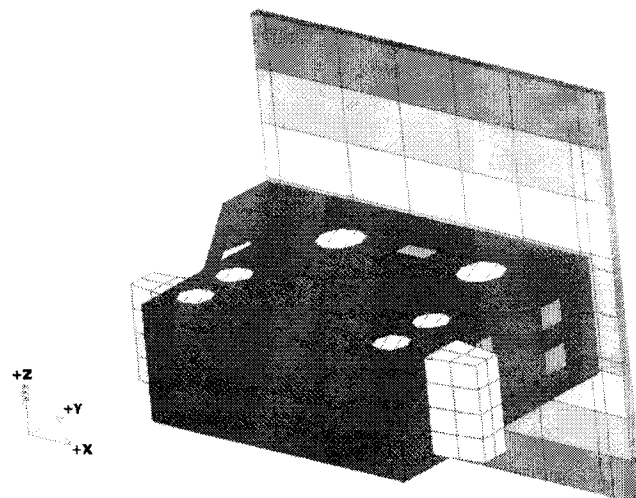

Figure 20. Optical bench with second stage radiator DTMM

Both the reduced and detailed models were run for the cold, hot, safe and survival cases. The models include logic to simulate heater circuits with thermostatic control. Orbital transient as well as orbit average steady state simulations were run. The orbit simulation showing only TES is illustrated in Fig. 23 when displayed from sun view.

ANALYSIS RESULTS

The analysis results show that the thermal control system meets all the specified temperature control requirements. In general, the results from both the reduced model and detailed model agree quite well. Typical results from the unit level detailed models are shown in Figs. 21 and 22.

Results from the orbital transient simulations with the reduced models are shown in Figs. 24-27. The hot case science mode results are shown in Figs. 24 and 25. A summary of the temperature predictions is shown in Table 7. Survival mode results are shown in Figs. 26 and 27. In this case, the radiator temperatures fall below the freezing point of ammonia, which is −78°C. The amount of heater power required to maintain the radiators above the freezing point of ammonia far exceeds the available survival power budget. For this

reason, propylene, which has a freezing point of −180°C and has the most flight heritage, was selected for the TES LHPs.

Results also show a 10% heat rejection margin for the second stage radiator and 15% margin for the first stage radiator of the passive cooler. These margins are acceptable at this stage of the instrument development life cycle.
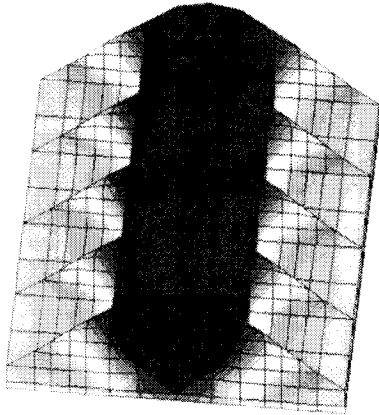

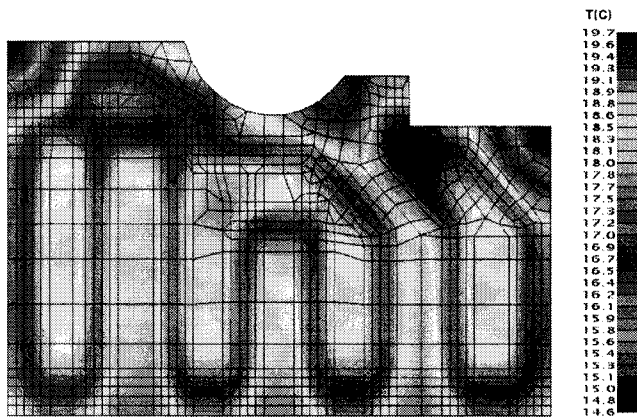Figure 21. IEM loop heat pipe evaporator detailed thermal

Figure 22. Electronics radiator detailed thermal model

CONCLUSIONS

Instrument and unit level thermal models have been developed for TES. These models have demonstrated that an acceptable thermal performance can be expected on orbit for all phases of the chemistry mission. The results presented show a robust thermal control design. Adequate temperature and power margins for all environmental conditions and instrument modes have been demonstrated. In the future, thermal balance test data from instrument-level thermal vacuum/ thermal

balance tests will provide the opportunity to verify the predicted temperature and power margins.

To date, an engineering model and proto-flight optical bench have been fabricated and delivered to JPL. Both units have passed static and dynamic testing at 1.25 times limit load.
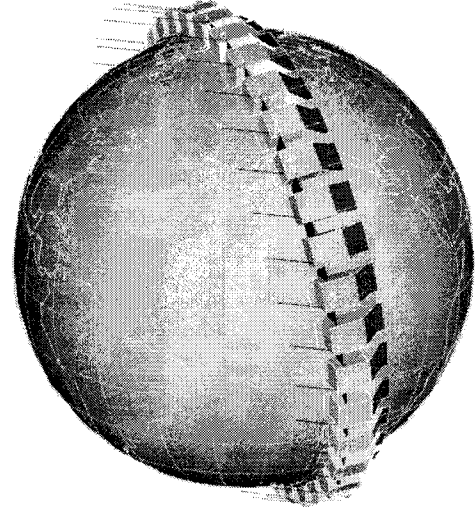

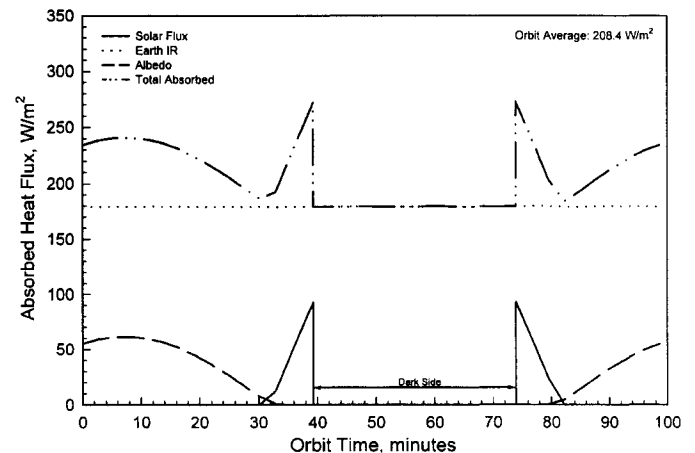Figure 23. Sun view of TES on orbit with Chemistry spacecraft removed: 36° beta angle

Figure 24. Nadir radiator orbital absorbed heat flux: hot case

The engineering model unit was populated with optics, aligned at room temperature, covered with an MLI blanket and a thermal shield and placed in a vacuum chamber for cooling down to its operating temperature at 180 K. Test results have demonstrated that the optical bench thermal design works by transferring the parasitic heat leaks to the second stage radiator, which rejected the heat to a liquid nitrogen cool shroud. The approach

10

to use composites for optical benches was validated by means of test results showing no detectable change in the alignment of the optics when checked at the operating temperature.

By end of fiscal year 2000, most of the flight hardware will have been delivered for integration into the instrument. Proto-flight instrument level thermal vacuum test is planned for June 2001 and the instrument will be delivered to the spacecraft integrator on December 2002.
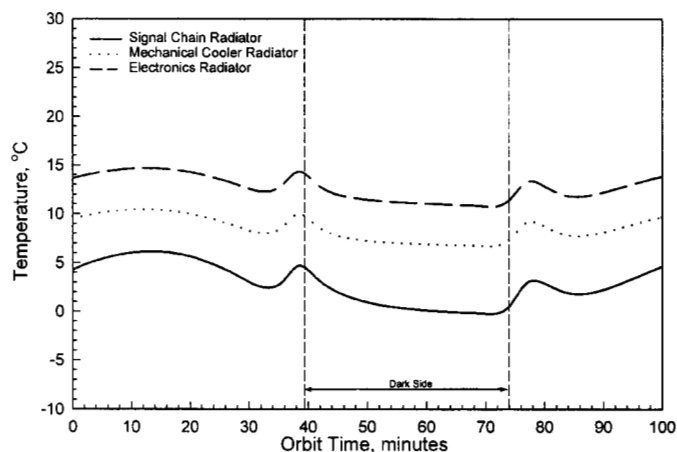

Figure 25. Nadir radiator orbital transient temperatures: hot case

Table 7. Flight temperature prediction summary

|	Flight Temperature Predictions (°C)				
	Operating				Non-operat Surv
	Cold Case		Hot Case		
	Orbit var.	Orbit ave.	Orbit var.	Orbit ave.	
IEM	0.3	7.8	1.0	20.6	0.6
Signal Chain Elect	0.1	4.8	0.3	17.3	-0.1
Cooler Electronics	0.2	8.4	0.4	20.8	1.1
Laser Head Elect	0.3	0.7	1.0	12.5	-0.3
Mech Cooler Compressor	0.3	4.6	1.1	15.3	18.4
Trans. Actuator/ Encoder	0.1	14.0	0.1	26.6	19.9
Roller Bearings	0.0	239.7K	0.0	247.3K	224.3K
Optical Bench (Optics Hsg)	0.1	176.0K	0.1	175.7K	203.8K
Filter Wheel	0.0	87.3K	0.0	88.4K	232.9K
Filter Wheel Act	0.0	-32.6	0.0	-20.3	42.4
Detectors	0.0	63.9K	0.0	64.0K	232.5K
Detector Pre-Amp	0.8	238.0K	0.9	243.6K	314.0K
Earth Shade Mech	0.5	0.0	0.5	11.7	0.1
PCS Roll Motor	0.1	2.5	0.4	16.8	27.1
PCS Pitch Motor	0.8	0.7	1.7	14.4	20.3
PCS Mirror	0.4	1.5	1.1	18.1	-11.9
Radiometric Calib.	0.1	4.0	0.2	17.4	-2.4
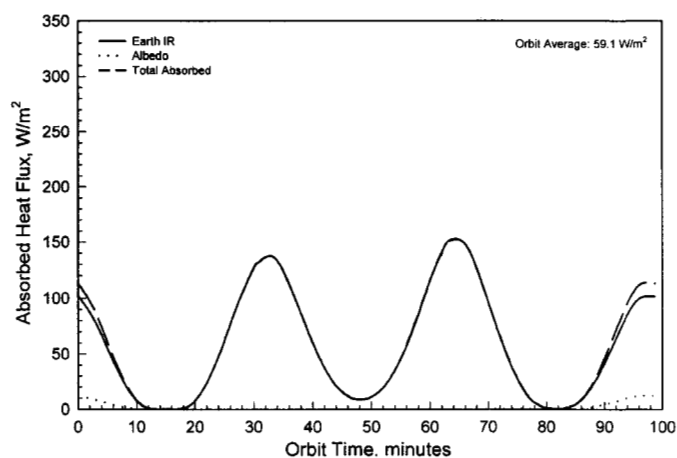
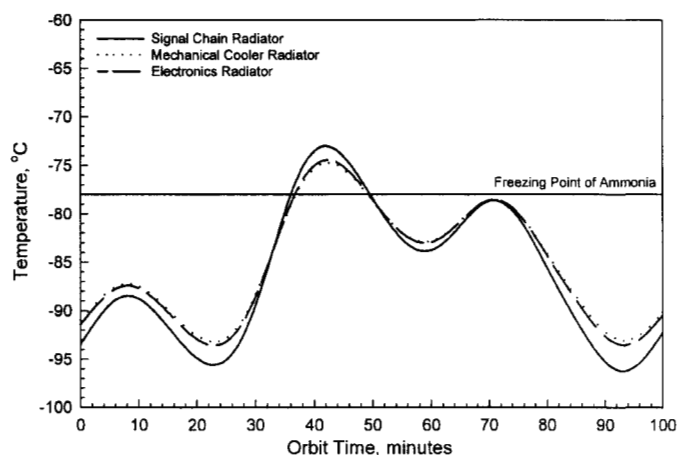Figure 26. Nadir radiator orbital absorbed heat flux: survival mode

Figure 27. Nadir radiator orbital transient temperatures: survival mode

REFERENCES

1. Ku, J., "Operating Characteristics of Loop Heat Pipes," SAE Paper No. 1999-01-2007, July 1999.
2. Sasin, V.Y., Zelenov, I.A., Zuev, V.G and Kotlyarov, E.Y., "Mathematical Model of a Capillary Loop Heat Pipe with a Condenser-Radiator," SAE Technical Paper Series, Paper No. 901276, July 1990.
3. Nikitkin, M., and Cullimore, B., "CPL and LHP Technologies: What are the Differences, What are the Similarities?," SAE Technical Paper Series, Paper No. 981587, July 1998.
4. Maidanik, Y.F., Fershtater, Y.G. and Solodovnik, N.N., "Loop Heat Pipes: Design, Investigation, Prospects of Use in Aerospace Technics," SAE Technical Paper Series, Paper No. 941185, April 1994.
5. Wolf, D.A., Ernst, D.M. and Phillips, A.L. "Loop Heat Pipes - Their Performance and Potential," SAE Technical Paper Series, Paper No. 941575, June 1994.
6. Maidanik, Y.F., et al., "Development and Experimental Investigation of Loop Heat Pipes," 7th International Heat Pipe Conference, 1990.
7. Maidanik, Y.F., Fershtater, Y.G., Pastukhov, V.G., Vershinin, S.V. and Goncharov, K.A., "Some Results of Loop Heat Pipes Development, Tests and Application in Engineering," 5th International Heat Transfer Symposium, Melbourne, Vic., 1996.
8. Maidanik, Y., Vershinin, S., Solodovnik, N., Gluck, D., and Gerhart, C., "Some Results of the Latest Developments and Tests of Loop Heat Pipes," 33rd Intersociety Energy Conversion Conference, LaGrange Park, IL, 1998.
9. Rodriguez, J.I., Pauken, M. and Na-Nakorpanom, A., "Transient Characterization of a Propylene Loop Heat Pipe during Startup and Shutdown," 30th SAE Technical Paper Series, Paper No. 00ICES-161, Toulouse, France, July 2000.
10. Pauken, M. and Rodriguez, J.I., "Performance Characterization and Model Verification of a Loop Heat Pipe," 30th SAE Technical Paper Series, Paper No. 00ICES-108, Toulouse, France, July 2000.
11. Glavich, T.A., and Beer, R., "Tropospheric Emission Spectrometer for the Earth Observing System," SPIE Proceedings, Vol. 1540, Bellingham, Washington, July 1991.

CONTACT

For additional information contact: Dr. Jose I. Rodriguez at the Jet Propulsion Laboratory. Phone:(818)354-0799. Email: Jose.I.Rodriguez@jpl.nasa.gov